

Supporting Information for: On the Atmospheric Fate of Methacrolein: 2. Formation of Lactone and Implications for Organic Aerosol Production

Henrik G. Kjaergaard^{1,}, Hasse C. Knap¹, Kristian B. Ørnsø¹, Solvejg Jørgensen¹,
John D. Crounse³, Fabien Paulot^{2,\$}, Paul O. Wennberg^{2,3,*}*

¹Department of Chemistry, University of Copenhagen, Universitetsparken 5, DK-2100
Copenhagen Ø, Denmark

²Division of Engineering and Applied Science, California Institute of Technology, Pasadena, CA
91125, USA

³Division of Geological and Planetary Sciences, California Institute of Technology, Pasadena,
CA 91125, USA.

^{\$} now with the Division of Engineering and Applied Sciences, Harvard University, Cambridge,
MA 02138, USA.

*To whom correspondence should be addressed. E-mail: hgk@chem.ku.dk. Phone: 45-35320334. Fax: 45-35320322. Email: wennberg@caltech.edu, Phone: 626-395-8655. Fax: 626-395-8535

Intrinsic Reaction Coordinate

The IRC shown in Figure S1 is produced from two different IRCs, and shows the reaction path from MPAN-OH via the M-TS transition state to form HMML + NO₃, and further via the E-TS transition state to HAC + CO + NO₃. The barrier height from MPAN-OH to M-TS is relatively small compared to the barrier height between HMML and E-TS. The deep well between the two transition states, may trap the HMML.

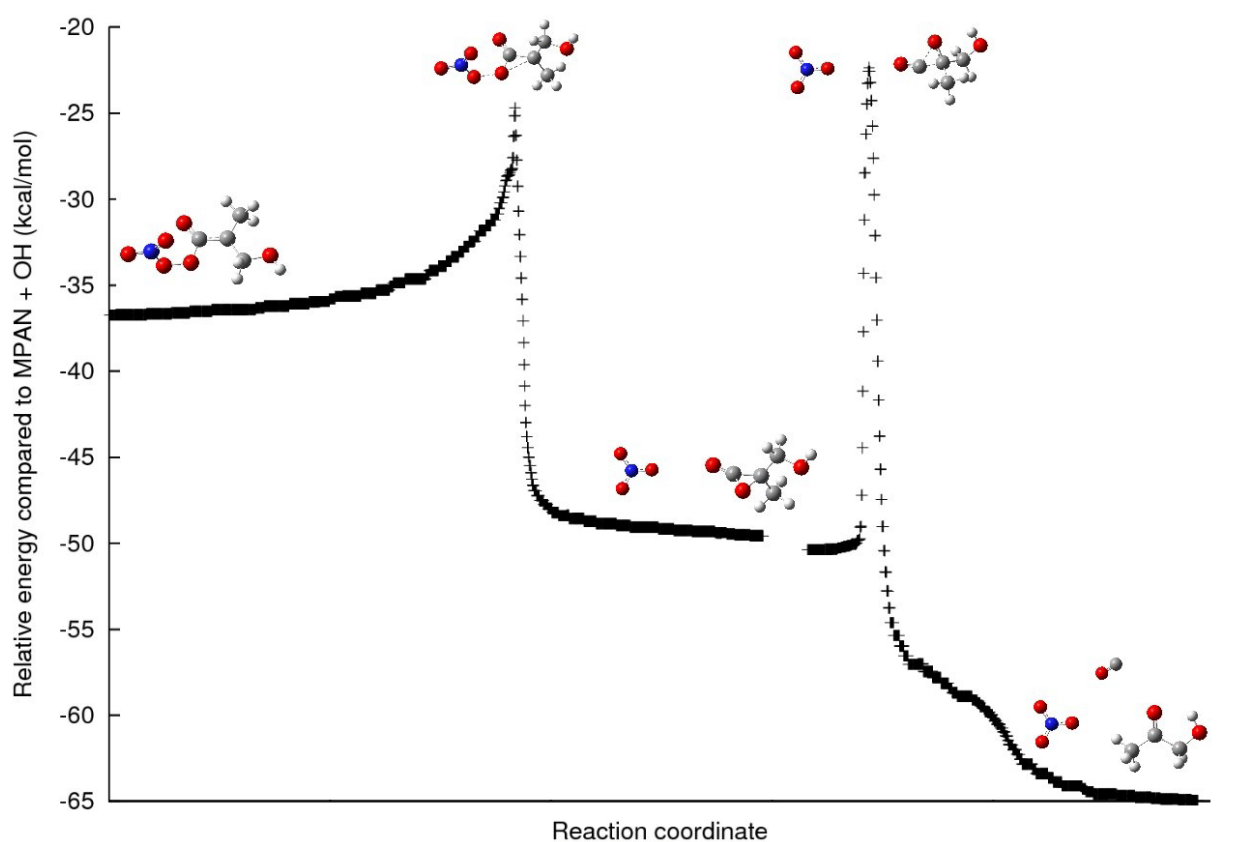


Figure S1. IRC path for the MPAN-OH to HAC + CO + NO₃ in relative energy difference from MPAN-OH. Two IRC paths calculated from the respective TS with the B3LYP/6-31+G(d,p) method without zero point vibrational energy correction.

Acrolein reactions

Reactions mechanisms for acrolein (CH_2CHCHO) following H-abstraction, similar to those for methacrolein (MACR) are shown in Figure S2.

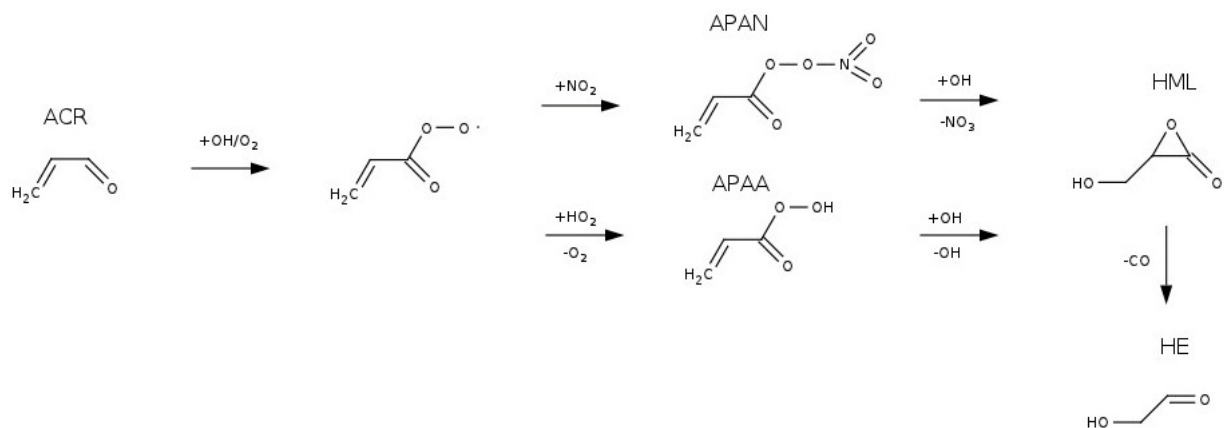


Figure S2. H-abstraction mechanism for the acrolein oxidation under high NO_x condition to form hydroxymethyl- α -lactone (HML). Additional abbreviations used: peroxyacryloyl nitrate (APAN), peroxyacrylic acid (APAA) and glycolaldehyde (HE).

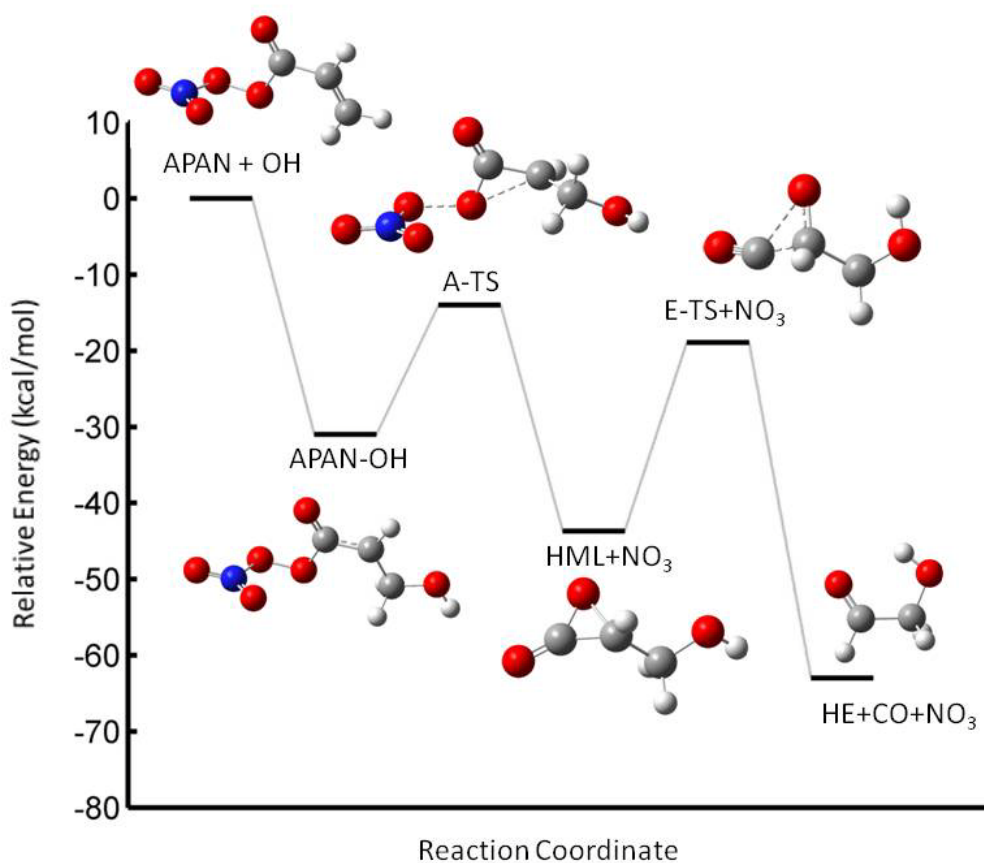


Figure S3. Relative energies for the reaction of APAN with OH with a loss of NO₃ to form hydroxymethyl- α -lactone (HML). The F12//B3LYP/aVTZ energies are corrected for zero point vibrational energy with the B3LYP/aVTZ harmonic frequencies. The B3LYP/aVTZ geometries for each of the stationary points are shown. HE is glycolaldehyde.

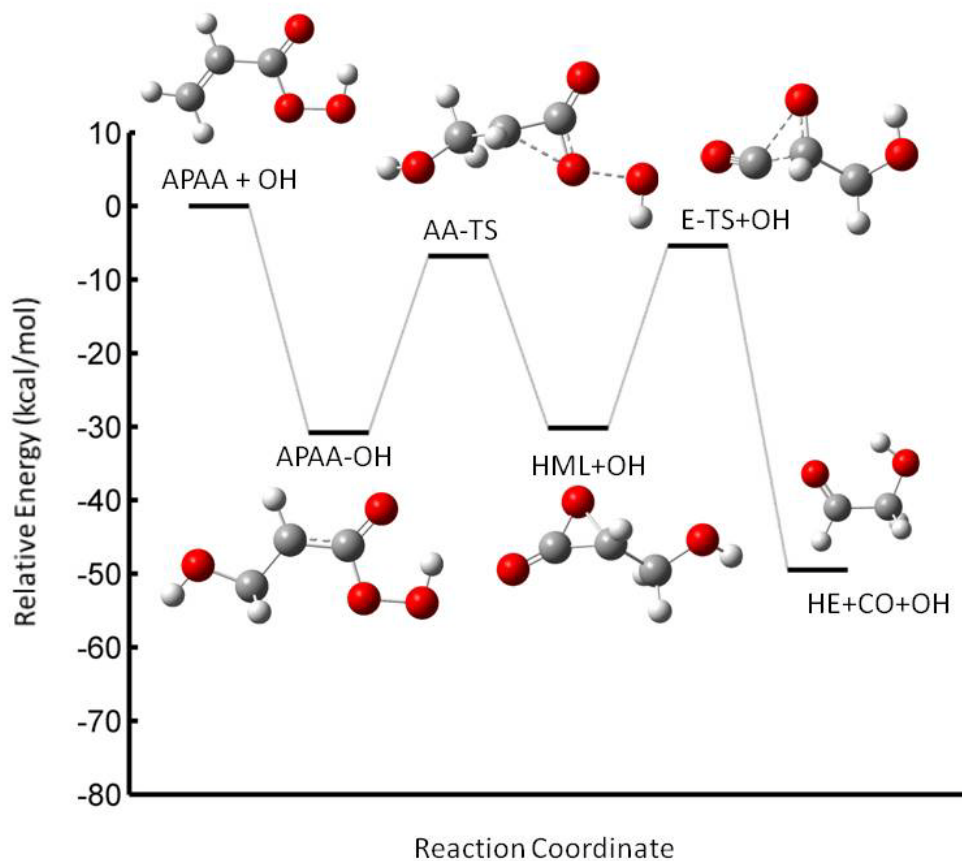


Figure S4. Relative energies for the reaction of APAA with OH with a loss of OH to form hydroxymethyl- α -lactone. F12//B3LYP/aVTZ energies are corrected for zero point vibrational energy with the B3LYP/aVTZ harmonic frequencies. The B3LYP/aVTZ geometries for each of the stationary points are shown. HE is glycolaldehyde.

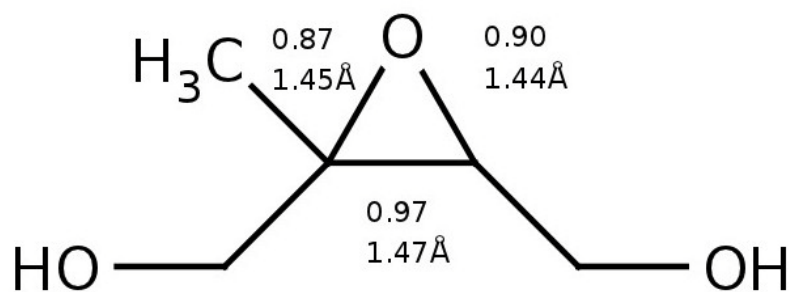


Figure S5. Dihydroxy-epoxide (IEPOX) with bond orders (top) and bond lengths (bottom) indicated for selected bonds.

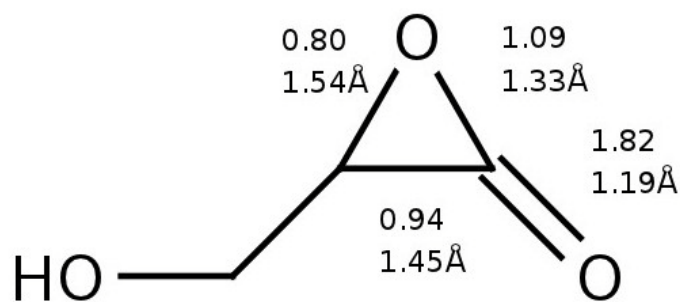


Figure S6. Hydroxymethyl- α -lactone (HML) with bond orders (top) and bond lengths (bottom) indicated for selected bonds.

TABLE S1: Energetics of the APAN + OH reaction (kcal/mol).

Compound	B3LYP/ 6-31+G(d,p) ^a	B3LYP/ aVTZ ^b	F12 ^b	ΔH^c	ΔG^c
APAN+OH	0.0	0.0	0.0	0.0	0.0
APAN-OH	-31.3	-30.2	-31.0	-32.0	-22.3
A-TS	-18.7	-17.0	-14.0	-14.9	-5.9
HML+NO ₃	-45.9	-45.5	-43.7	-44.3	-46.7
E-TS+ NO ₃	-20.6	-22.4	-18.9	-19.5	-22.0
HE+CO+NO ₃	-61.9	-62.7	-63.0	-62.5	-75.9
A-TS $\tilde{\nu}_{IMAG}$ (cm ⁻¹)	542i	569i	-	-	-
E-TS $\tilde{\nu}_{IMAG}$ (cm ⁻¹)	418i	380i	-	-	-

^a Including B3LYP/6-31+G(d,p) ZPVE correction.

^b Including B3LYP/aug-cc-pVTZ ZPVE correction.

^c F12 energies and B3LYP/aug-cc-pVTZ thermal correction at 298.15K.

TABLE S2: Energetics of the APAA + OH reaction (kcal/mol).

Compound	B3LYP/ 6-31+G(d,p) ^a	B3LYP/ aVTZ ^b	F12 ^b	ΔH^c	ΔG^c
APAA+OH	0.0	0.0	0.0	0.0	0.0
APAA-OH	-31.1	-30.0	-30.8	-31.8	-22.2
AA-TS	-11.2	-9.9	-6.8	-7.3	1.0
HML+OH	-28.2	-28.0	-30.2	-31.7	-31.6
E-TS+OH	-2.9	-5.0	-5.4	-5.5	-5.4
HE+CO+OH	-44.2	-45.3	-49.5	-48.5	-59.3
A-TS $\tilde{\nu}_{IMAG}$ (cm ⁻¹)	561i	577i	-	-	-
E-TS $\tilde{\nu}_{IMAG}$ (cm ⁻¹)	418i	380i	-	-	-

^a Including B3LYP/6-31+G(d,p) ZPVE correction.

^b Including B3LYP/aug-cc-pVTZ ZPVE correction.

^c F12 energies and B3LYP/aug-cc-pVTZ thermal correction at 298.15K.

Estimate of yields.

We have estimated the yield of the intermediates and products in the investigated reactions (e.g. MPAN + OH) with a RRKM master equation analysis using the MultiWell 2011 program suite.[1-3] We have used collisional Lennard-Jones potentials for MPAN-OH (and other reactants) and HMML with parameters from similar sized molecules, naphthalene and methylcyclohexane, respectively.[4] The collisions are assumed to be with O₂. Collisional activation and deactivation is included according to the generalized exponential model for toluene, with $\alpha(E) = 0.1243 \text{ kcal/mol} + 0.0042E$ and $\gamma = 0.7$. [2,5] For all the calculations, unless otherwise stated, we have used the default settings and T = 298 K, P = 1 atm and Ntrials = 100000. The Ntrials = 100000 gives a convergence of about 0.2% for these reactions. We have not included tunneling or centrifugal correction. We assume irreversible reactions and assume that we have fast internal vibrational energy redistribution. In our calculations all energies are F12/aVTZ with zero-point corrections from B3LYP/aVTZ. The starting energy of MPAN-OH has been distributed thermally by MultiWell. The excess energy of the leaving fragment NO₃ (OH) is assumed to be 3 kcal/mol, which includes the rotational (1 kcal/mol), [6] vibrational (1 kcal/mol – thermal average) and translational energy (3/2 kT ~ 1 kcal/mol).

TABLE S3: Yields for the different channels.

R	R-OH	HMML/HML	HAC/HE
MPAN	2%	61%	36%
MPAA	83%	17%	0.2%
APAN	21%	15%	64%
APAA	89%	10%	0.8%

TABLE S4: Varying excess energy of leaving NO₃ fragment.

E(NO ₃) (kcal/mol)	MPAN-OH	HMML	HAC
3	2%	61%	36%
4	2%	66%	32%
5	2%	70%	27%
6	2%	74%	23%

TABLE S5: Varying the temperature in the model.

T (K)	MPAN-OH	HMML	HAC
248	9%	72%	19%
298	2%	61%	36%
348	0.5%	44%	55%

References:

- [1] MultiWell-2011 Software, 2011, designed and maintained by John R. Barker with contributors Nicholas F. Ortiz, Jack M. Preses, Lawrence L. Lohr, Andrea Maranzana, Philip J. Stimac, T. Lam Nguyen, and T. J. Dhillip Kumar; University of Michigan, Ann Arbor, MI; <http://aoss.engin.umich.edu/multiwell/>.
- [2] Barker, J. R.; *Int J Chem Kinet*, **2001**, *33*, 232-245.
- [3] Barker, J. R., *Int. J. Chem. Kinet*, **2009**, *41*, 748-763.
- [4] Cuadros, F., Cachadina, I., Ahumada, W., *Molec. Engineering*, **1996**, *6*, 319-325.
- [5] Barker, J. R.; Ortiz, N. F.; *Int J Chem Kinet*, **2001**, *33*, 246-261.
- [6] Matthews, J.; Sinha, A.; Francisco, J. S.; *J. Chem. Phys.* **2005**, *112*, 221101.